Dyna
ISSN: 0012-7353
dyna@unalmed.edu.co
Universidad Nacional de Colombia
Colombia

Garzón, Carlos Mario; Alfonso, José Edgar; Corredor, Edna Consuelo
Characterization of adherence for Ti6Al4V films RF magnetron sputter grown on stainless steels
Dyna, vol. 81, núm. 185, junio, 2014, pp. 183-189
Universidad Nacional de Colombia
Medellín, Colombia

Available in: http://www.redalyc.org/articulo.oa?id=49631031026

- How to cite
- Complete issue
- More information about this article
- Journal's homepage in redalyc.org

redalyc.org
Scientific Information System
Network of Scientific Journals from Latin America, the Caribbean, Spain and Portugal
Non-profit academic project, developed under the open access initiative

UNIVERSIDAD NACIONAL DE COLOMBIA
SEDE MEDELLÍN
FACULTAD DE MINAS

DYNA

http://dyna.medellin.unal.edu.co/

# Characterization of adherence for Ti6Al4V films RF magnetron sputter grown on stainless steels
# Caracterización de la adherencia para películas de Ti6Al4V depositadas por medio de pulverización catódica magnetrón RF sobre acero inoxidable

Carlos Mario Garzón [a], José Edgar Alfonso [b] & Edna Consuelo Corredor [c]

[a] *Departamento de Física, Universidad Nacional de Colombia sede Bogotá, Colombia. cmgarzono@unal.edu.co*
[b] *Departamento de Física, Universidad Nacional de Colombia sede Bogotá, Colombia. jealfonsoo@unal.edu.co*
[c] *Facultad de Ingeniería, Universidad Libre de Colombia, Colombia. ednaconsueloc@gmail.com*

Received: May 5th, 2013. Received in revised form: January 31th, 2014. Accepted: May 16th, 2014.

**Abstract**
Ti6Al4V films were grown on UNS S31600 austenitic stainless steel samples by RF magnetron sputtering. On top of samples, macroindentation tests were carried out to characterize the film to substrate adherence according to the recommended VDI 3198 procedure. Sputter deposition experiments varying both chamber pressure and target applied power were carried out. All films displayed superior adhesion to the substrates. A non-monotonic relationship between adherence and chamber pressure or target applied power was observed. The lowest adherences were associated with intermediate pressures and powers. The outstanding film to substrate adherence was mainly addressed to monophasic and nanometric film character (crystallite size was roughly 20 ± 10 nm) and to rather high continuity and homogeneity of films.

*Keywords:* Thin films, Nanostructures, Biomaterials, RF-Magnetron sputtering.

**Resumen**
El acero inoxidable UNS S31600 fue recubierto con películas de la aleación Ti6Al4V, por medio de la técnica pulverización catódica magnetrón rf. La superficie de los materiales obtenidos se sometió a ensayos de macroindentación, de acuerdo con el procedimiento VDI 3198, para caracterizar la adherencia película-sustrato. Se realizaron experimentos de depósito variando tanto la presión del gas al interior de la cámara de depósito como la potencia aplicada al blanco. La adherencia película-sustrato varío no monotónicamente con la presión y la potencia; la menor adherencia se observó para las presiones y las potencias intermedias. En términos generales se observó una excelente adherencia película-sustrato, la cual se atribuyó principalmente al carácter nanométrico de los cristalitos de las películas (diámetro promedio alrededor de 20 ± 10 nm), a su carácter monofásico y a su elevado grado de uniformidad tanto química como morfológica.

*Palabras Clave:* Películas delgadas, Nanoestructuras, Biomateriales, Pulverización catódica magnetrón rf.

## 1. Introduction

Nowadays, the supply of low-cost prosthesis for replacing bones in humans, like the ones in artificial hips, is deficient. That negatively impacts life quality of poor people in countries with weak public health systems, like many of the countries in Latin America. Consequently, several research groups in the region had already been carried out works where microstructure optimization of materials in surgical appliances and prostheses was targeted [1,2].

Austenitic stainless steels, titanium alloys, and hidroxiapatita are widely employed for the production of prosthesis due to their low cost, good levels of biological compatibility, good bioactive response or high mechanical strength [1-10].

However, manufacture of volumetric bone replacements, like the ones in artificial hips, using only any one of the above referenced materials (austenitic stainless steels, titanium alloys, and hidroxiapatita), and simultaneously observing all the positive properties required in that uses, is not possible. Every one of the depicted materials displays serious drawbacks among the claimed properties. Stainless steels are not biologically active, and their biological compatibility is restricted; titanium alloys are rather expensive, and their levels of biological activity are rather restricted and; finally, hidroxiapatita is not as tough as it is necessary in that kind of surgical appliances and prostheses.

Recent progresses in surface engineering and materials science have triggered the development of a wide variety of technical processes for manufacturing multi-structure materials, where these new materials have mechanical, tribological, or other functional properties that cannot be

© The authors; licensee Universidad Nacional de Colombia.

achieved from the individual traditional materials alone. In those multi-structure materials, chemical and mechanical properties vary locally from material surface toward material inner regions. The main example of these multi-structure materials are those materials obtained by deposition of customized films on traditional substrates [9-12].

Traditional materials coated with thin films can be tailored to exhibit high levels of overall toughness, high tribological performance in different tribo-systems, and high levels of biological compatibility. Unfortunately, these materials coated with thin films have sharp variations in their mechanical properties and consequently are prone to decohesion at the region of transition between film and substrate due to local adherence failure.

Decohesion failures can be triggered by low levels of film to substrate adherence, high levels of residual stresses at the region near to the surface, and deformation incompatibilities due to local steep variations in the stress–strain relationships.

Low levels of film to substrate adherence can be induced by inadequate preparation of surface substrate during material processing, contamination of substrate surfaces prior to film deposition or low adherence levels regarding the crystal lattices of both film and substrate (the so-called intrinsic adherence). Thus, it is common that the same class of film grown on two different substrates presents different levels of adhesion, even if all the processing parameters are unmodified [13,14]. It has also been reported that very different levels of film to substrate adhesion could be obtained after grow TiN, Ti(C,N) and TiAlN films on the same steel but with different periods of precleaning the substrate surface with plasma ions [13].

There exist diverse standardized and non-standardized experimental procedures for assessing film to substrate adherence [14,15]. Unfortunately, these tests give results concerning film to substrate adherence that actually are performance parameters where several others factors but not only the intrinsic adherence are involved [14,15]. Thus, *a priori*, results on film to substrate adherence obtained from different types of tests are not totally interchangeable [15,16].

The following can be listed as the most frequently used adherence tests: scratch, four-points bending, cavitation due to ultrasonic vibration in a fluid (commonly water), impact, macroindentation, acoustic microscopy and laser-acoustic wave attenuation [15].

In adherence tests by macroindentation, a hardness indentation on top of samples is carried out and later evaluation in the microscope of damaged regions is done [16,17]. This is a destructive test, which is fast and reliable, as well as easy to do in almost every materials science facility equipped for mechanical properties evaluation.

Recommended procedure VDI 3198 reports guidelines for performing macroindentation adherence tests [16,17].
In this paper, it is depicted an experimental research dealing with magnetron sputtering deposition of Ti6Al4V thin (around 1 □m in tick) films on a conventional austenitic stainless steel and latter characterization of film to substrate adherence by macroindentation, following the recommended procedure VDI 3198. The aim of this research was to study the effect of variations on both target applied power and pressure inside the vacuum chamber, on film to substrate adherence for materials obtained. A discussion on the effects of film integrity on film to substrate adherence is also presented.

Table 1. Chemical composition (wt-%) of the materials.

| | Cr | Ni | Mn | Si | Mo | C | Fe | Ti | Al | V |
|---|---|---|---|---|---|---|---|---|---|---|
| UNS S31600 Steel | 18.5 | 9.5 | 2.0 | 0.85 | 2.0 | 0.03 | Bal. | - | - | - |
| Titanium target | - | - | - | - | - | - | - | Bal. | 6.0 | 4.0 |

## 2. Materials

Samples of the austenitic stainless steel UNS S31600, in the annealed condition, were used as substrate material.

For the target material the titanium alloy Ti6Al4V was used. A commercially available alloy that has impurity levels lower than 0.01 wt-%, was used.

Table 1 gives the chemical composition of both, substrate and target, materials.

## 3. Experimental procedures

### *3.1. Growth of Ti6Al4V films by magnetron sputtering*

Thin films (around 1 μm thick) of titanium alloy Ti6Al4V were grown on samples of UNS S31600 steel through RF magnetron sputtering, using an Alcatel HS 2000 apparatus, which consists of an RF magnetron and a deposition chamber evacuated using both mechanical and turbo-molecular pumps. The equipment is implemented with gas mixer, gas flux controller, and pressure controller.

Deposition experiments varying both pressure inside the vacuum chamber (between 0.002 and 0.05 mbar) and target applied power (between 200 and 500 W) were carried out. In these experiments, neither external heating of substrate nor external applied voltage (bias) were used.

Prior to film deposition, steel substrates were sputter cleaned for 10 min using plasma power of 200W. This stage of sputter cleaning was performed with the aim of removing oxide layers at the steel surface, mainly the passive film.

### *3.2. Characterization of test samples*

Both, phase identification and determination of crystallite size were carried out by X-ray diffraction experiments, using a Philips PW 1710 conventional diffractometer.

X-ray experiments were carried out with monochromatic radiation Cu K-α, λ= 1.54056 Å, generator voltage of 40

kV and generator current of 30 mA. The X-ray irradiation length was 5 mm.

Phase identification was made using diffraction patterns obtained from XRD scans where the angular step was 0.02°, the swept time was 2 s and the scanning Bragg angles, 2θ, were varied from 20° to 90°. Collected XRD patterns were compared to theoretical X-ray polycrystalline patterns filed by the ICDD (International Center Diffraction Data).

Crystallite size measurements were made following a Scherrer analysis, using diffraction patterns obtained from XRD scans where the angular step was 0.02°, the swept time was 20 s and the scanning Bragg angles, 2θ, were varied from 33° to 42°. It was aimed at to record diffraction peaks corresponding to the crystallographic planes (110) from the BCC titanium phase.

Morphology and spatial distribution of defects in films were evaluated by examining sample surfaces in a scanning electron microscope. A Philips XL30 conventional microscope was used. Experiments of electron microscopy were carried out varying the acceleration voltage between 15 and 25 kV and the working distance between 8 and 15 mm.

Chemical composition of films was assessed by EDS microanalysis (Energy-dispersive X-ray spectroscopy), using the same scanning electron microscope referred. Four EDS measurements on top of each sample were performed.

Film thicknesses were assessed by profilometry measurements.

Film hardness was measured by carrying out indentation hardness tests on top of samples. These hardness experiments were carried out in a nanohardness tester coupled to an atomic force microscope. A diamond-tip Berkovitch indenter was used with a maximum load of 5 mN. The low indentation load (5 mN) aimed at to avoid substrate effects on the results of film hardness. Twelve indentations in each sample were made, and results reported are the outcome of a statistical analysis of that twelve data for sample.

### *3.3. Film to substrate adherence*

Film to substrate adherence was assessed by means of macroindentation tests, carried out according to VDI 3198 recommended procedure [16,17]. Several indentation imprints were made on top of each sample and then damage inside and around the imprints was evaluated using micrographs obtained in the scanning electron microscope.

Indentation experiments were carried out using a diamond-tip Otto Wolpert-Werke indenter and indentation load of 150 kg-f. Five indentations were made in each sample, being the distance between them carefully set larger than ten times the indentation length. It is worth noting that these indentation parameters are the ones used in Rockwell-C hardness tests.

VDI 3198 indentation tests allowed the assessment of a set of HF indexes that specify the level of film to substrate adherence. Those adherence indexes can be assessed by comparison of appearance of damage at indented surfaces with a series of standardized damage patterns presented in Fig. 1 in the paper of Vidakis et al. [17]. As a result of such comparison, a HF index is assigned to the specific film – substrate pair. These indexes range from HF1 to HF6, where lower HF values are associated to better film to substrate adherences. According to Vidakis et al. [17], HF1 to HF4 indexes are related to good enough adhesion levels while HF5 and HF6 indexes are indication of poor film to substrate adherence.

## 4. RESULTS

### *4.1. Characterization of test samples*

All samples showed almost the same chemical composition. Chemical composition of the films was around 7.0 ± 1.0 Al wt-%, 3.0 ± 1.0 V wt-% and balance Ti. Heterogeneities in chemical composition at different regions of the sample, if they actually exist, were lower than the detection limit (1.0 wt-%) of EDS microanalysis for the conditions of this study.

Profilometry measurements showed that film thicknesses were around 1 μm: film thicknesses ranging between around 0.8 μm and 1.5 μm were detected. An analysis on the effect of variations of deposition parameters, namely target applied power and chamber pressure, on film thickness was not appraised because scattering of film thicknesses data were close to thickness variations aimed to detect.

Fig. 1 shows the diffraction patterns obtained for two representative samples. patterns for the other samples are similar to these two in Fig. 1, and they are not shown for simplicity. After visual juxtaposition of obtained X-ray diffraction patterns (Fig. 1) with polycrystalline theoretical patterns filed by the ICDD, it was identified the Ti-β (BCC) phase. On the other hand, *a priori*, X-ray diffraction patterns allowed to state that the films were virtually free of both Ti-α (HC) phase and amorphous phase.

Scanning electron microscopy (SEM) results showed that the films are rather continuous, in despite of some porous observed. Heterogeneous distributions of porous, with area fraction concentrations lower than 0.1 area-%, with cylindrical, polygonal, and irregular shapes were observed, like these shown in Fig. 2. The size of these porous varied between 1.0 and 4.0 μm equivalent diameter.

The results on average crystallite size, average hardness, and HF adherence index are given in Tables 2 and 3. Crystallite sizes referenced in those tables are the average diameters of crystallites XRD-estimated with regard to the crystallographic planes (110) of Ti-β phase. These crystallite sizes were computed following a Scherrer analysis.

Average crystallite sizes between 10 and 25 nm were measured. Strong variations in crystallite size were induced when the power applied to target was varied, while modifications in the chamber pressure induced only mild variations in that crystallite size. Higher powers and lower pressures induced coarser crystallites.

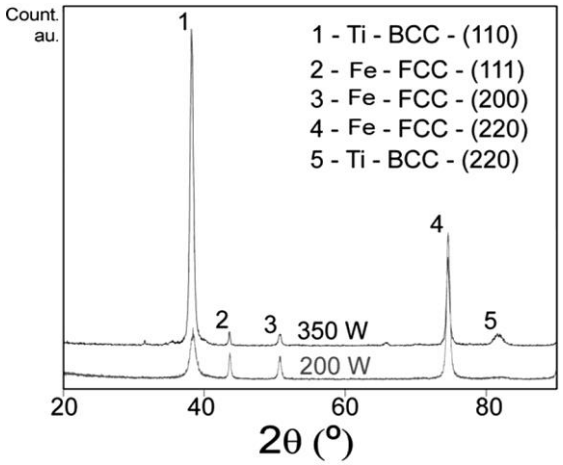


Figure 1. Diffraction patterns for two representative samples.

Excepting one set of samples, average film hardness was not sensitive to variations in the deposition parameters, average film hardness was around 10.0 GPa. In samples obtained with chamber pressure of 5×10-3 mbar and target applied power of 350 W, the average hardness was 8.5 GPa. Hardness distribution histograms for data collected in each sample are shown in Fig. 3. Even though average hardness was very close in all samples (excepting one set of samples), every sample displayed a distinctive hardness distribution histogram. That heterogeneity in hardness values inside each sample could be addressed not to actual different levels of hardness in different microregions but to variations in distribution and size of defects. This relationship between statistical distribution of hardness and defect concentration will be also discussed in this article.

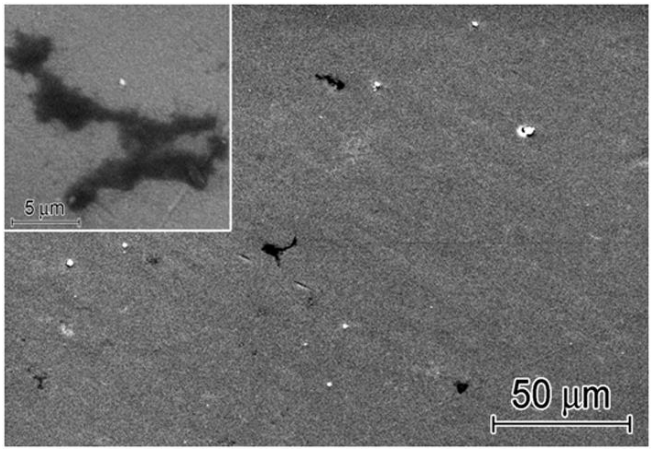


Figure 2. On top surface general aspect for a sample processed at 350 W – 0.005 mbar. SEM photograph.

Table 2. Main features of samples processed with $5\times10^{-3}$ mbar chamber pressure.

| Power (W) | Crystallite size (nm) | Hardness (GPa) | Adherence index HF (dimensionless) |
|---|---|---|---|
| 200 | 11±1.5 | 10.4±0.7 | HF1 |
| 350 | 16.5±2 | 8.5±0.6 | HF3 |
| 500 | 24.1±3.5 | 10.3±0.6 | HF1 |

Table 3. Main features of samples processed with 350 W target applied power.

| Pressure (mbar) | Crystallite size (nm) | Hardness (GPa) | Adherence index HF (dimensionless) |
|---|---|---|---|
| $2\times10^{-3}$ | 15.4±2 | 10.1±0.3 | HF1 |
| $5\times10^{-3}$ | 16.6±2 | 8.5±0.6 | HF3 |
| $5\times10^{-2}$ | 10.6±1 | 10.4±0.5 | HF3 |

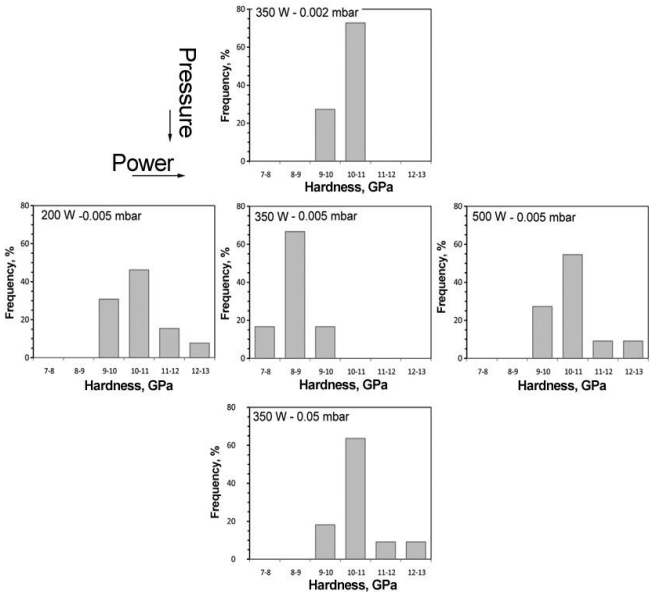


Figure 3. Hardness level distribution histogram.

### *4.2. Film to substrate adherence*

Fig. 4 shows, for each sample, three SEM micrographs corresponding to three different indentation imprints. SEM micrographs were taken at ×200 magnification, which is the recommended magnification in VDI 3198 procedure (refer Section 3.3). After comparing the five indentation imprints (only three of them are shown in Fig. 4) for each sample, not significant differences were detected. That is interpreted in this work as high reproducibility levels of adherence tests.

Comparison of micrographs in Fig. 4 and damage charts on VDI 3198 procedure (Fig. 1 in the paper of Vidakis *et al.* [17]) allows stating that all samples exhibited high adherence levels: classifications HF1 and HF3.

Fig. 4 allows to conclude that variations in deposition parameters, namely power and pressure, induced significant variations of adherence levels. That is interpreted in this work as high detectability level of adherence tests.

In Fig. 4 a non-monotonic relationship between adherence and chamber pressure or target applied power could be pointed out, where the poorest adherences can be associated to intermediate pressures and/or powers (insets b and c in Fig. 4).

Fig. 5 shows SEM micrographs of damaged regions took at ×1000 and ×5000 magnifications. Representative micrographs are shown; however reproducibility levels were high, as it was mentioned.

High magnification SEM micrographs in Fig. 5 allow pointing that the main mechanisms of damage were: crack propagation, plastic deformation, and debris detachment.

Cracking patterns are a powerful qualitative result that encloses rich information on film to substrate adherence [14,17]; however, their interpretation is not straightforward. In Fig. 5, after analyzing the periphery of imprints, one can see both crack propagation in the axial direction and debris detachment, being these two damage traces less intense as better is film to substrate adhesion. Samples with the highest levels of film adherence (Fig. 5, insets a and d) show mild cracking patterns and scarce debris detachment at both regions, imprint periphery and imprint inner regions.

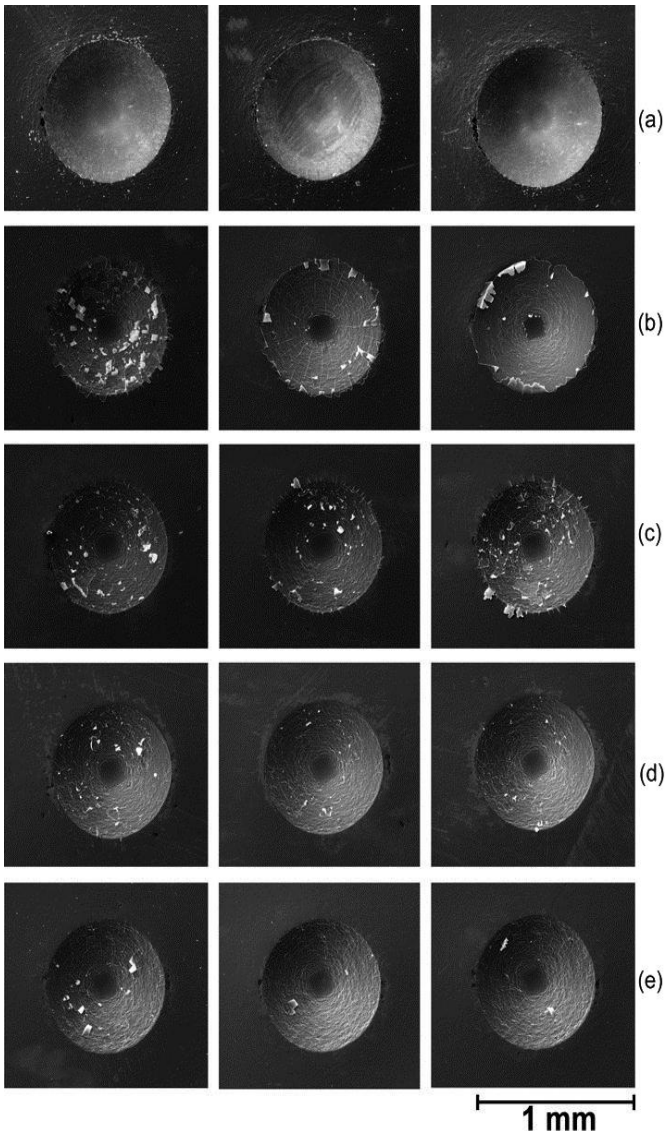


(a) $2\times10^{-3}$ – 350 W; (b) $5\times10^{-3}$ – 350 W; (c) $5\times10^{-2}$ – 350 W; (d) $5\times10^{-3}$ – 500 W; (e) $5\times10^{-3}$ – 200 W.
Figure 4. SEM micrographs at ×200 magnification taken on top of samples after macroindentation tests.

Generally, all samples displayed an intense pattern of sleep lines following circular directions of imprints. However, not significant crack growth in those circular directions was observed. The accentuated patterns of sleep lines arise from intense plastic deformation of substrate steel (which is ductile and soft). That intense plastic deformation of substrate imposes a high stress level to films, which are hard and do not display significant ductility. Thus, the fact that only minor cracking was observed in the circular directions of imprints is a key evidence of high film to substrate adherence.

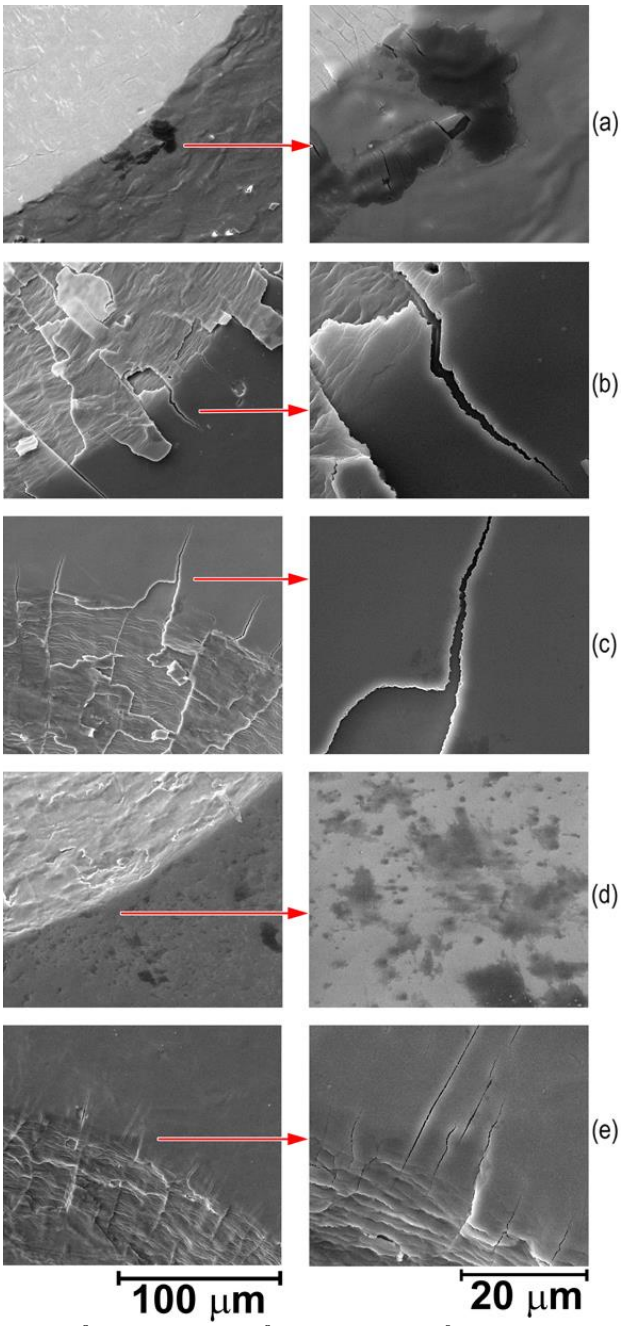


(a) $2\times10^{-3}$ – 350 W; (b) $5\times10^{-3}$ – 350 W; (c) $5\times10^{-2}$ – 350 W; (d) $5\times10^{-3}$ – 500 W; (e) $5\times10^{-3}$ – 200 W.
Figure 5. SEM micrographs at ×1000 and ×5000 magnification taken on top of samples after macroindentation tests.

## 5. Discussion

Superior levels of film to substrate adherence were obtained, even though film hardness was very high (around 10 GPa) with regard to the hardness of the substrate (around 1.6 to 1.8 GPa).

It can be deduced that high elasto-plastic constrains are imposed to films during the indentation process. That is because of both, step hardness variations in the regions of transition from film to substrate and high levels of plastic deformation of substrate (substrates are ductile and soft). In spite of those high elasto-plastic constrains, it was observed that a net brittle character of the film failure was not induced. In Fig. 5, there are even traces of ductile behavior of films (i.e., propagation of deformation inside films in a plastic mode), which is viable because of the metallic character of films. This film ductility differs from the one distinctive brittle behavior of hard films composed of titanium nitrides or carbides [14].

The observed combination of hard and tough character of films can be addressed to their monophasic and metallic character as well as to the nanometer character of film structures.

It was pointed out in this work that crystallite size variations did not lead to significant variation in hardness, being film hardness almost insensitive to changes of deposition parameters. In addition, the monophasic and metallic character of films is not expected to notably vary among the diverse samples (with experimental results as a basis). From those annotations a virtual wrong conclusion could be formulated: it should be expected that variations in deposition parameters induce very small changes in film to substrate adherence. However, experimental results showed a sharp variation of adherence when deposition parameters were varied, mainly when the target applied power was changed. To elucidate this virtual misunderstanding, it is essential to correlate results presented in Fig. 3 to 5. This correlation between spread of individual hardness values inside each sample and film to substrate adherence allows to conclude that those films where the hardness distribution histogram was sharper (Fig. 3 - pressure $2\times10^{-3}$ mbar and power 350 W) are the films displaying better adherence levels in Fig. 4 and 5. The mentioned homogeneity in hardness histograms inside some samples can be addressed to low concentration of defects, and *vice versa*, defect concentrations are high in films which show high spreads in their individual hardness values, or even lessened hardness averages (pressure = $5\times10^{-3}$ mbar and power = 350 W & pressure = $5\times10^{-2}$ mbar and power = 350 W).

As it was stated, while deposition parameters where varied, film to substrate adherence underwent significant variations. Both, high reproducibility and high detectability character of the tests, allowed noticing even smooth variations in adherence. As a matter of fact, regarding to the six adherence levels reported in VDI 3198, in this work it was possible to detect smoother adherence variations among samples where the HF index was constant. In Fig. 4, one can see that samples obtained with 200 W – $5\times10^{-3}$ mbar, 500 W – $5\times10^{-3}$ mbar and 350 W – $2\times10^{-3}$ mbar exhibit the same adherence level HF1, whereas combining Fig. 4 and 5, it can be stated that among these three sets of sample the ones obtained with pressure = $2\times10^{-3}$ mbar and power = 350 W are the samples with the highest adherence level while samples obtained with 500 W – $5\times10^{-3}$ mbar have associated the poorest adherence of this group of three samples. As lower was the level of film to substrate adherence, micrographs with more pronounced axial cracking and more evidence of debris detachment were obtained. After comparing samples displaying HF3 adherence index (pressure = $5\times10^{-3}$ mbar and power = 350 W & pressure = $5\times10^{-2}$ mbar and power = 350 W), it is also possible to state that from the two groups, the samples processed with 350 W – $5\times10^{-3}$ mbar display lower adherence levels. In conclusion, indentation tests and SEM detailed analysis of damage allowed to classify in a very individualized ranking the film to substrate adherence, with a more gradable classification that the one proposed in VDI 3198 procedure.

Results presented about hardness, morphological and chemical continuity of the films and film to substrate adherence, when analyzed in the light of results in literature [10-14] show that materials in this research are adequate for using in surgical appliances and prostheses where high wear resistance, high toughness, and high ductility are a must. Due to the bulk part of these materials is composed of a conventional stainless steel and the outmost part is composed of a titanium alloy, it can be expected that these materials should be not expensive and can display moderate levels of biocompatibility. Although the core material has not high levels of biocompatibility, both the high continuity of films and its high level of wear resistance avoid the possibility that body tissues and fluids keep in contact with the steel, inhibiting the flux of dangerous metallic ions (e.g., ions of nickel) from the material to the body.

## 6. Conclusions

Experiments assessing macroindentation adherence of Ti6Al4V films grown on stainless steel by RF magnetron sputtering were carried out. Analysis of results from this experiment revealed that deposition procedures depicted in this work are suitable for obtaining Ti6Al4V films highly adherent to steel substrates.

Among the major factors inducing the high levels of film to substrate adherence, the following can be listed: small size of crystallites (around 20 ± 10 nm), monophasic film character (BCC), metallic character of both the film and the substrate and, finally, rather high continuity and homogeneity of films.

Indentation experiments allowed detecting even small differences in film to substrate adherence produced by chamber pressure or target applied power variations; the poorest adherences being associated to intermediate pressures and/or powers.

The major factor inducing variations in film to substrate adherence was hardness heterogeneities inside each sample,

being that hardness heterogeneities a result of defect distributions in the films: the sharper the distribution of hardness values the better the adherence.

## References

[1] García, C., Paucar, C. y Gaviria, J. Estudio de algunos parámetros que determinan la sintesis de hidroxiapatita por la ruta de precipitación. Dyna, 148, pp 9-15, 2006.

[2] Copete, H., Lopez, M., Vargas, F., Echavarría, A. y Rios, T. Evaluación del comportamiento in vitro de recubrimientos de hidroxiapatita depositados mediante proyección térmica por combustión oxiacetilénica sobre un sustrato de Ti6Al4V. Dyna, 177, pp 101-107, 2013.

[3] Anselme, K., Noel, B. and Hardouin, P. Human Osteoblast Adhesion on Titanium Alloy, Stainless Steel, Glass and Plastic Substrates with Same Surface Topography. J. Materials Science-Mater. Med., 10, pp815-819, 1999.

[4] Balazic, M., Kopac, J., Jackson, J. M. and Ahmed, W. Titanium and Titanium Alloy Applications in Medicine. Int. J. of Nano and Biomaterials, 1, pp 3-34, 2007.

[5] Dorozhkin, S.V. Bioceramics Based on Calcium Orthophosphates, Glass and Ceramics. 64, pp 442-447, 2007.

[6] Niinomi, M. Mechanical Biocompatibilities of Titanium Alloys for Biomedical Applications. J. Mechanical Behaviour of Biomedical Materials, 1, pp 30-42, 2008.

[7] Miura, K., Yamada, N., Hanada, S., Jung, T. and Itoi, E. The bone tissue compatibility of a new Ti-Nb-Sn alloy with a low Young's modulus. Acta Biomaterialia, 7, pp 2320-2326, 2011.

[8] Yilmazer, H., Niinomi, M., Nakai, M. Cho, K. Hieda, J., Todaka, Y. and Miyazaki, T. Mechanical properties of a medical β-type titanium alloy with specific microstructural evolution through high-pressure torsion. Materials Science and Engineering C, 33, pp 2499–2507, 2013.

[9] Lee, C., Chua, J., Chang, W., Lee, J., Jangc, J. and Liawd, P. Fatigue property improvements of Ti–6Al–4V by thin film coatings of metallic glass and TiN: a comparison study. Thin Solid Films, in press, corrected proof, disponible en linea (http://dx.doi.org/10.1016/j.tsf.2013.08.027) 14 August 2013.

[10] Zalnezhad, E., Baradaran, S., Bushroa, R. and Sarhan, A. Mechanical Property Enhancement of Ti-6Al-4V by Multilayer Thin Solid Film Ti/TiO2 Nanotubular Array Coating for Biomedical Application. Metallurgical and Materials Transactions A, 45A, pp 785-797, 2014.

[11] De Souza, G., De Lima, G., Kuromoto, N., Soares, P., Lepienski, C., Foerster, C. and Mikowski, A. .Tribo-mechanical characterization of rough, porous and bioactive Ti anodic layers. Journal of the mechanical behavior of biomedical materials, 4, pp 796-806, 2011.

[12] Erişir, E., Suadiye, E. and Gümüş, S. Microstructural characterization of wear of Arc-PVD Ti and Ti6Al4V coated austenitic stainless steels in Ringer's solution, Proceedings of 3rd International Conference of Engineering Against Failure (ICEAF III), pp. 421-427, 2013.

[13] Zoestbergen, E. and De HOSSON, J. Crack Resistance of PVD Coatings: Influence of Surface Treatment Prior to Deposition, Surface Engineering, 18, pp 283-288, 2002.

[14] Heinkea, W., Leylanda, A., Matthewsa, A., Bergb, G., Friedrichb, C. and Broszeitb, E. Evaluation of PVD nitride coatings, using impact, scratch and Rockwell-C adhesion tests, Thin Solid Films, 270, pp 431-438, 1995.

[16] VDI - Verein Deutscher Ingenieure, Procedimiento 3198: Beschichten von Werkzeugen der Kaltmassivumformung; CVD- und PVD-Verfahren, Alemania, 1992.

[15] Ollendorf, H. and Schneider, D. A comparative study of adhesion test methods for hard coatings, Surface and Coatings Technology, 113, pp 86-102, 1999.

[17] Vidakisa, N. Antoniadis, A. and Bilalis N. The VDI 3198 indentation test evaluation of a reliable qualitative control for layered compounds, Journal of Materials Processing Technology, pp 143-144, 481-485, 2003.

## Acknowledgements

This work was financially supported by "Dirección de Investigación, DIB" at the National University of Colombia and "Colciencias". Structural support was also provided by the "Centro Internacional de Física, CIF", Physics Department of National University of Colombia and Metallurgical and Materials Engineering Department of University of São Paulo (Brazil).

**C.M. Garzón**, received the Bs. Eng in Mechanical Engineering in 1994 from the Universidad Nacional de Colombia. He earned a MS degree (2001) and a PhD degree (2004) both in Metallurgical and Materials Engineering from the Universidade de São Paulo, Brazil. He has attended two full-time postdoctoral positions, one of them at the Brazilian Synchrotron Light Laboratory in Campinas (Brazil), 2005-2006, and the other one at the Grenoble Institute of Technology in Grenoble (France), 2008-2009. He started his academic carrier as a full professor at the Universidad de Ibagué in 1998, where he worked by two years. Currently he is a full professor at the Physics Department of the Universidad Nacional de Colombia, Bogotá. His research work has been focused on Materials Science and Engineering, in the realm of metallic materials processing and properties.

**J. E. Alfonso**, completed his Bachelor's degree in Physics in 1987 and his Master's degree in Science - Physics in 1991, both of them being obtained from the Universidad Nacional de Colombia. In 1997 he completed his PhD in Science -Physics at the Universidad Autonoma de Madrid (Spain). He has been linked to the Universidad Nacional de Colombia as a full professor since 2000, where his research has been focused on material science, particularly on thin film processing as well as performance characterization, studying thin film optical, electrical and mechanical properties.

**Edna Consuelo Corredor**, completed her Bachelor's degree in Physics from the Universidad Pedagogica y Tecnologica de Colombia in 2005. In 2009 she obtained her Master's degree in Physics and Physical Technologies and, in 2012 completed her PhD in Physics, both at the University of Zaragoza, Zaragoza, Spain. Currently, she is a full professor in the Science Division, Department of Engineering, Universidad Libre de Colombia. Her research focuses on: the structural and corrosion studies of metallic thin films grown on stainless steel substrates and, on the other hand, the preparation and characterization of magnetic nanostructures with potential application in high density recording media, magnetic sensors and magnetic actuators.